

## Galactic and extragalactic hydrogen in the X-ray spectra of Gamma Ray Bursts

I.I. Rácz<sup>1,2</sup>, Z. Bagoly<sup>1</sup>, L.V. Tóth<sup>1,2</sup>, L.G. Balázs<sup>1,2</sup>, I. Horváth<sup>3</sup> and S. Pintér<sup>1</sup>

<sup>1</sup> *Eötvös University*

*Pázmány Péter sétány 1/A, H-1117 Budapest, Hungary*

*(E-mail: racz@complex.elte.hu)*

<sup>2</sup> *MTA CSFK Konkoly Observatory*

*Konkoly Thege Miklós út 15-17, H-1121 Budapest, Hungary*

<sup>3</sup> *National University of Public Service*

*Ludovika tér 2, H-1083 Budapest, Hungary*

Received: April 30, 2017; Accepted: June 18, 2017

**Abstract.** Two types of emission can be observed from gamma-ray bursts (GRBs): the prompt emission from the central engine which can be observed in gamma or X-ray (as a low energy tail) and the afterglow from the environment in X-ray and at shorter frequencies. We examined the Swift XRT spectra with the XSPEC software. The correct estimation of the galactic interstellar medium is very important because we observe the host emission together with the galactic hydrogen absorption. We found that the estimated intrinsic hydrogen column density and the X-ray flux depend heavily on the redshift and the galactic foreground hydrogen. We also found that the initial parameters of the iteration and the cosmological parameters did not have much effect on the fitting result.

**Key words:** Gamma-ray bursts – X-rays: general

### 1. Introduction

Gamma-ray bursts (GRBs) are powerful explosions that have been observed in the distant Universe. The GRBs are observed at all wavelengths, from gamma-rays to radio (Amati et al., 2013; Mészáros et al., 2014). The duration of GRBs is characterized by the  $T_{90}$  which is the time taken to accumulate 90% of the total observed counts. It seems that there are 3 groups of GRBs in duration: short, intermediate, and long which have  $T_{90} \approx 0.3$  s,  $T_{90} \approx 8.5$  s, and  $T_{90} \approx 40$  s, respectively (Horváth et al., 2008, 2010). The long GRBs (LGRBs) are tracers of star formation and as such may indicate large structures in the Universe. The Hercules-Corona Borealis Great Wall was found by Horváth et al. (2014, 2015) and the Giant GRB Ring was found by Balázs et al. (2015).

We can distinguish twotypes of emission, the prompt emission from the central engines and the afterglow emission from the environment. The former can be observed in gamma and X-rays (as a low energy tail, sometimes, called X-ray

flash), the latter between X-rays and radio (Kumar & Zhang, 2015). The prompt emission refers to the operation of the central engine and the afterglow provides information about the local, intergalactic and galactic medium (Starling et al., 2013). There are many parameters that can be calculated from the radiation of the central engine as its duration, peak flux, fluence and/or about the properties of the environment such as the hydrogen column density.

The *Swift* space telescope (Barthelmy et al., 2005; Burrows et al., 2005; Roming et al., 2005) detected  $\geq 1270$  GRBs until 20th April (2017). The *Swift* *BAT*, *XRT* and *UVOT* observe the outbursts in gamma, X-ray and ultraviolet/optical respectively. The radiation leaving the GRB travels through the intergalactic and galactic foreground which significantly affects the spectrum we observe (Evans et al., 2007). This is the reason why it is necessary to subtract the foreground so that we can gather adequate information about the medium around the GRB.

The galactic foreground is not as homogeneous as we have previously thought (Toth et al., 2017). It seems to be heavily structured and clumpy which makes accurate measurement difficult. The resolution of the methods used - which are based on the radio surveys of atomic hydrogen - are of the order of magnitude of degrees, therefore clumps much smaller than this can not be observed with these measurements.

In this paper we analyze how the observed X-ray spectra of GRBs depend on the hydrogen foreground. We also examine the dependence on cosmology parameters, redshift, and the initial parameters of the iteration.

## 2. *Swift* XRT data

There are several space observatories dedicated to the study of GRBs. In this article we use only the data obtained from the *Swift* satellite. *Swift* has three instruments on-board working together to observe GRBs and their afterglows from gamma across X-rays to optical wavebands.

The X-ray Telescope (XRT) can take simple images, light curves and spectra of the GRB afterglow. This instrument provides a more precise location of the GRBs with a typical error circle of approximately 2 arcseconds radius. The telescope has an energy range of 0.2 - 10 keV, but it is normally used in the 0.3 - 10.0 keV energy range (Hill et al., 2004). The XRT has 3 operating modes depending on the flux and the instrument changes automatically depending on the observed intensity. In this work we also used the Windowed Timing (WT) mode and Photon Counting (PC) mode spectra. The WT data has a 1.7-millisecond time resolution and does one-dimensional imaging and the PC has a 2.5-second time resolution and does two-dimensional imaging. Both modes work in the full energy resolution which is approximately 260 eV. The XRT spectra

were created from the event data by HEASARC HEASOFT<sup>1</sup>, which we could download from the *Swift* data center.

Many of the physical parameters of GRBs can be calculated from the light curves and spectra as well. The hydrogen column density of the local environment or redshift can be obtained from the spectra.

### 3. Spectral fitting

At least one spectrum is made by the automatic *Swift* procedure: a time-averaged spectrum which is available in the archive servers. If the GRB is observable for more than 4 ks after the trigger, a further late-time spectrum is made. For statistical analysis we examined the time-averaged spectra.

For fitting the X-ray spectra we used the XSPEC software which is a widely used interactive X-ray spectra fitting program (Arnaud, 1996; Dorman & Arnaud, 2001; Dorman et al., 2003). We can set many parameters like cosmological or solar abundances and use some models constructed from individual components.

#### 3.1. Classic method

An automatic method to analyze Swift XRT spectra from the UK Swift Science Data Center (UKSSDC) was published by Evans et al. (2009). The UKSSDC uses the initial settings and properties listed below:

- 0.3-10.0 keV energy range
- Standard flat Universe cosmology parameters ( $H_0 = 70 \frac{\text{km}}{\text{Mpc}\cdot\text{s}}$ ,  $q_0 = 0.0$ ,  $\Lambda_0 = 0.73$ )
- Low metallicity interstellar medium abundance from Wilms et al. (2000)
- Photoelectric absorption cross-section from Verner et al. (1996)
- A powerlaw ('powerlaw'), a flux convolution model ('cflux') and two ISM absorption models from Wilms et al. (2000) ('(z)TBabs') in which one constant is galactic and the other is fittable intrinsic. Figures 1 and 2 show some of the theoretical model spectra with different hydrogen column densities and different redshift settings
- All types of redshift data with photo-z values
- Estimation of the galactic foreground from the Leiden-Argentine-Bonn (LAB) Survey of Galactic HI survey (Kalberla et al., 2005) where the best resolution was  $> 20$  arcsec

---

<sup>1</sup><https://heasarc.nasa.gov/lheasoft/>

### 3.2. Improved fitting

We examined how setting different galactic hydrogen column densities and different redshifts influence the X-ray spectral models.

Figure 1 shows the dependence of the shape of the X-ray afterglow spectrum on the local column density. The break point appears at a higher energy level increasing with the column density.

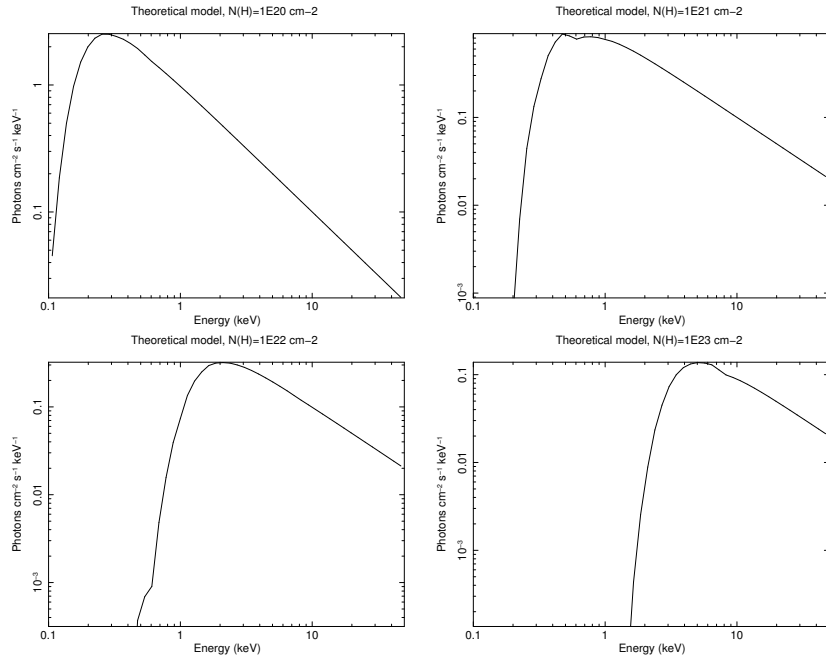


**Figure 1.** Top-left, top-right, bottom-left, bottom-right plots show model X-ray spectra for a local hydrogen column density of  $10^{20} \text{ cm}^{-2}$ ,  $10^{21} \text{ cm}^{-2}$ ,  $10^{22} \text{ cm}^{-2}$ ,  $10^{23} \text{ cm}^{-2}$ , respectively.

In Figure 2 we show the effect of redshift variation with the absorbing layer. A special configuration is also shown with two absorbing layers, one local (in our galaxy) and one remote. The hydrogen column density of the remote layer is extremely high in our example, larger than in a typical GRB host galaxy but still not unrealistic.

Furthermore, we tried to improve the fitting and in the meantime we used unified settings and models in order to obtain comparable results. We used the `cflux*TBabs*zTBabs*powerlaw` model with fixed initial parameters. The initial intrinsic column density was  $0.0 \text{ cm}^{-2}$ , the flux was  $10^{-12} \text{ erg cm}^{-2} \text{ s}$  and the initial powerlaw index was 1.0.

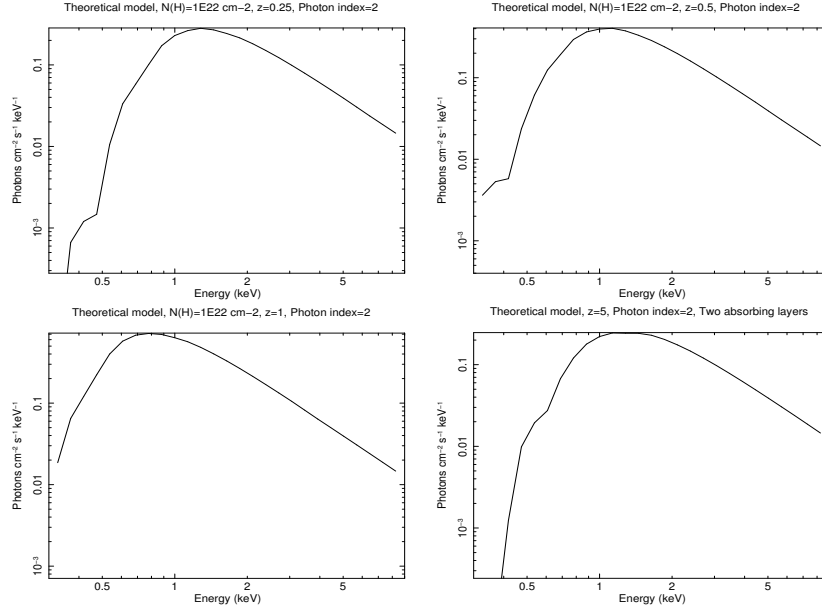


**Figure 2.** Top-left, top-right, bottom-left plots show model X-ray spectra assuming an absorbing layer with a hydrogen column density of  $10^{22} \text{ cm}^{-2}$  at a redshift of  $z = 0.25$ ,  $z = 0.5$ ,  $z = 1$ , respectively. The bottom-right plot shows a model X-ray spectrum with two assumed absorbing layers, with hydrogen column density of  $5 \cdot 10^{21} \text{ cm}^{-2}$  and  $10^{23} \text{ cm}^{-2}$  and redshift of  $z = 0$  and  $z = 5$  respectively. The applied photon index was 2.0 for all the four models.

Finally, we used as the best values of redshift the ones obtained from the spectral fitting procedure. Here we checked every redshift measurement and skipped the photo-redshift data, and we kept only the afterglows or host galaxies spectroscopic redshifts.

If the redshift was unknown we set it to 0.0. Figure 3 shows our fitting results. Here we changed the galactic foreground and used only the reliable spectroscopic redshift values which were obtained from afterglows and host galaxies' spectra. The finally obtained best fit is preferable because the Chi-square improved from 478.1 to 476.315 for 382 degrees of freedom. we see a slight improvement with our taken last solution that can be also seen by naked eye.

## 4. Conclusions

We examined the reliability of the results by starting the fitting from different initial parameters, for example extragalactic column densities or flux. We found that the fitted flux and power indices are absolutely not sensitive parameters,

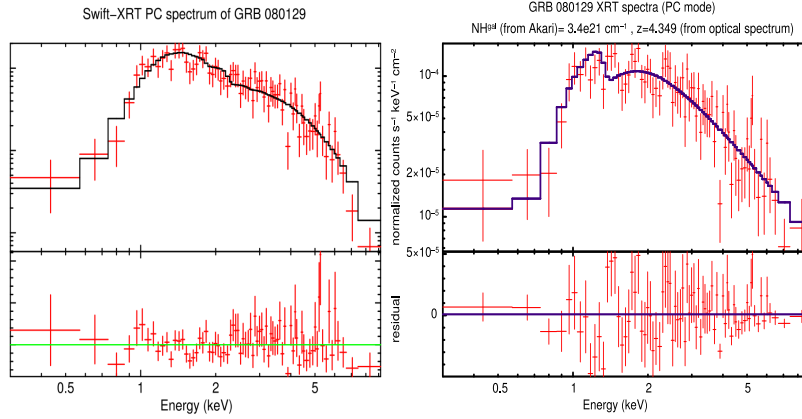


**Figure 3.** Time-averaged spectra of GRB080129 with the best fits. On the left side we can see the 'catalog' spectrum fit from the UKSSDC, on the right side there is our X-ray spectral fit. We changed the input foreground column density and the redshift and we found a significant difference in the intrinsic column density.

however, the intrinsic column density might vary up to one order of magnitude. Even the new galactic foreground can change the intrinsic column density not negligibly and can also modify the photon index.

We made the fitting with different cosmological constants but the results were not sensitive to small changes. Furthermore, we found that the X-ray flux and intrinsic column density depend heavily on the redshift value.

## 5. Summary

The gamma-ray bursts are observed at all wavelengths, from gamma-rays to radio. There are two types of emission, the prompt emission from the central engine which can be observed in gamma or X-rays and the afterglow from the environment in X-ray and at shorter frequencies. Many parameters can be calculated about the central engine as well as about the environment, as the intrinsic column density. The prompt emission refers to the operation of the central engine and the afterglow shows the local and intergalactic and galactic medium as the hydrogen column density.

We examined the Swift XRT spectra with the XSPEC software. We used only the time-averaged spectra in this work. The correct estimation of the galactic interstellar medium is very important because we observe only the total flux and we need to subtract the absorption of the galactic gas from it. The intrinsic hydrogen column density may also vary several orders of magnitude by changing

the galactic foreground component. This intrinsic column density and the X-ray flux depend heavily on the redshift. We also found that the fitting results were not significantly sensitive on the initial parameters and the cosmological parameters.

We found that the precise redshift and galactic foreground values are essential parameters in the X-ray spectral fitting of GRBs.

**Acknowledgements.** This work was supported by the Hungarian OTKA NN-111016 grant. This work made use of data supplied by the UK Swift Science Data Centre at the University of Leicester. We acknowledge the use of public data from the Swift data archive.

## References

- Amati, L., Atteia, J.-L., Balazs, L., et al. 2013, *White paper*, arXiv:1306.5259
- Arnaud, K. A. 1996, in *Astron. Soc. of the Pacific Conf. Ser.*, Vol. 101, *Astron. Data Anal. Soft. and Sys. V*, ed. G. H. Jacoby & J. Barnes, 17
- Balázs, L. G., Bagoly, Z., Hakkila, J. E., et al. 2015, *Mon. Not. R. Astron. Soc.*, **452**, 2236
- Barthelmy, S. D., Barbier, L. M., Cummings, J. R., et al. 2005, *Space Sci. Rev.*, **120**, 143
- Burrows, D. N., Hill, J. E., Nousek, J. A., et al. 2005, *Space Sci. Rev.*, **120**, 165
- Dorman, B. & Arnaud, K. A. 2001, in *Astron. Soc. of the Pacific Conf. Ser.*, Vol. 238, *Astron. Data Anal. Soft. and Sys. X*, ed. F. R. Harnden, Jr., F. A. Primini, & H. E. Payne, 415
- Dorman, B., Arnaud, K. A., & Gordon, C. A. 2003, in *Bulletin of the American Astronomical Society*, Vol. 35, *AAS/High Energy Astrophysics Division #7*, 641
- Evans, P. A., Beardmore, A. P., Page, K. L., et al. 2007, *Astron. Astrophys.*, **469**, 379385
- Evans, P. A., Beardmore, A. P., Page, K. L., et al. 2009, *Mon. Not. R. Astron. Soc.*, **397**, 1177
- Hill, J. E., Burrows, D. N., Nousek, J. A., et al. 2004, in *SPIE Proceedings*, Vol. 5165, *X-Ray and Gamma-Ray Instrumentation for Astronomy XIII*, ed. K. A. Flanagan & O. H. W. Siegmund, 217–231
- Horváth, I., Bagoly, Z., Balázs, L. G., et al. 2010, *Astrophys. J.*, **713**, 552
- Horváth, I., Bagoly, Z., Hakkila, J., & Tóth, L. V. 2015, *Astron. Astrophys.*, **584**, A48
- Horváth, I., Balázs, L. G., Bagoly, Z., & Veres, P. 2008, *Astron. Astrophys.*, **489**, L1
- Horváth, I., Hakkila, J., & Bagoly, Z. 2014, *Astron. Astrophys.*, **561**, L12
- Kalberla, P. M. W., Burton, W. B., Hartmann, D., et al. 2005, *Astron. Astrophys.*, **440**, 775
- Kumar, P. & Zhang, B. 2015, *Physics Reports*, **561**, 1

- Mészáros, P., Asano, K., & Veres, P. 2014, in Journal of Physics Conference Series, Vol. 485, Journal of Physics Conference Series, 012001
- Roming, P. W. A., Kennedy, T. E., Mason, K. O., et al. 2005, *Space Sci. Rev.*, **120**, 95
- Starling, R. L. C., Willingale, R., Tanvir, N. R., et al. 2013, *Mon. Not. R. Astron. Soc.*, **431**, 31593176
- Toth, L. V., Doi, Y., Zahorecz, S., et al. 2017, *Publication of Korean Astronomical Society*, **32**, 113
- Verner, D. A., Ferland, G. J., Korista, K. T., & Yakovlev, D. G. 1996, *Astrophys. J.*, **465**, 487
- Wilms, J., Allen, A., & McCray, R. 2000, *Astrophys. J.*, **542**, 914